Tunable single-mode photonic lasing from zirconia inverse opal photonic crystals

Yoshiaki Nishijima[1], Keisei Ueno[1], Saulius Juodkazis[1], Vygantas Mizeikis[1], Hiroaki Misawa[1], Mitsuru Maeda[2], and Masashi Minaki[2]

[1] *Research Institute for Electronic Science (RIES), Hokkaido University, CRIS Bldg., Kita 21 Nishi 10, Kita-ku Sapporo 001-0021, Japan*

[2] *Sanyo Chemical Industries, Ltd., Ichinohashinomotocho 11-1,Higasiyama-ku Kyoto 605-0995, Japan*

Corresponding author:misawa@es.hokudai.ac.jp.

Abstract: Lasing from zirconia inverse opal photonic crystal structures infiltrated by solutions of rhodamine dyes was found to exhibit single-mode lasing peaks with spectral width less than 1 nm and quality factor in excess of 4000. The lasing occurs within the approximate range of high-reflectance spectral region associated with photonic stop band along ⟨111⟩ crystallographic direction, but its wavelength is not fixed to the corresponding Bragg wavelength of the periodic structure, and depends on the spectral position of the gain band. This lasing regime can be useful for realizing tunable single-mode photonic crystal lasers.

OCIS codes: (160.5298) Photonic crystals; (140.2050) Dye Lasers; (160.3380) Laser materials;

References and links

1. E. Yablonovitch, "Inhibited Spontaneous Emission in Solid-State Physics and Electronics," Phys. Rev. Lett. **58**, 2059–2062 (1987).
2. S. John, "Strong localization of photons in certain disordered dielectric superlattices," Phys. Rev. Lett. **58**, 2486–2489 (1987).
3. J. D. Joannopoulos, S. G. Johnson, J. N. Winn, and R. D. Meade, *Photonic Crystals: Molding the Flow of Light* 2nd ed. (Princeton University Press, Princeton and Oxford, 2008).
4. N. A. Clark, A. J. Hurd, and B. J. Ackerson, "Single colloidal crystals," Nature **281**, 57–60 (1979).
5. H. Fudouzi and Y. Xia, "Photonic papers and inks: color writing with colorless materials," Adv. Mater. **15**, 892–896 (2003).
6. H. Fudouzi, "Fabricating high-quality opal films with uniform structure over a large area." J Colloid. Interface Sci. **275**, 277–283 (2004), http://dx.doi.org/10.1016/j.jcis.2004.01.054.
7. A. Blanco, E. Chomski, S. Grabtchak, M. Ibisate, S. John, S. Leonard, C. Lopez, F. Meseguer, H. Miguez, J. Mondia, G. Ozin, O. Toader, and H. van Driel, "Large-scale synthesis of a silicon photonic crystal with a complete three-dimensional bandgap near 1.5 micrometres," Nature **405**, 437–40 (2000).
8. S. A. Rinne, F. García-Santamaría, and P. V. Braun, "Embedded cavities and waveguides in three-dimensional silicon photonic crystals," Nature Photon. **2**, 52 – 56 (2008).
9. L. Bechger, P. Lodahl, and W. L. Vos, "Directional fluorescence spectra of laser dye in opal and inverse opal photonic crystals." J Phys. Chem. B **109**, 9980–9988 (2005), http://dx.doi.org/10.1021/jp047489t.
10. A. Brzezinski, J.-T. Lee, J. D. Slinker, G. G. Malliaras, P. V. Braun, and P. Wiltzius, "Enhanced emission from fcc fluorescent photonic crystals," Phys. Rev. B (Condensed Matter and Materials Physics) **77**, 106 (2008), http://link.aps.org/abstract/PRB/v77/e233106.
11. F. Jin, Y. Song, X.-Z. Dong, W.-Q. Chen, and X.-M. Duan, "Amplified spontaneous emission from dye-doped polymer film sandwiched by two opal photonic crystals," Appl. Phys. Lett. **91**, 031109 (2007), http://link.aip.org/link/?APL/91/031109/1.

#99396 - $15.00 USD Received 25 Jul 2008; accepted 17 Aug 2008; published 20 Aug 2008

12. S. Frolov, Z. Vardeny, A. Zakhidov, and R. Baughman, "Laser-like emission in opal photonic crystals," Opt. Commun. **162**, 241–246 (1999).
13. M. N. Shkunov, M. C. DeLong, M. E. Raikh, Z. V. Vardeny, A. Zakhidov, and R. H. Baughman, "Photonic versus random lasing in opal single crystals," Synthetic Metals **116**, 485 – 491 (2001).
14. S. Furumi, H. Fudouzi, H. Miyazaki, and Y. Sakka, "Flexible polymer colloidal-crystal lasers with a light-emitting planar defect," Adv. Mater. **19**, 2067–2072 (2007).
15. F. Jin, C.-F. Li, X.-Z. Dong, W.-Q. Chen, and X.-M. Duan, "Laser emission from dye-doped polymer film in opal photonic crystal cavity," Appl. Phys. Lett. **89**, 241,101 (2006).
16. V. S. Letokhov, "Generation of light by a scattering medium with negative resonance absorption," Sov. Phys. JETP **26**, 835 – 840 (1968).
17. D. Wiersma, M. van Albada, and A. Lagendijk, "Coherent backscattering of light from an amplifying medium," Phys. Rev. Lett. **75**, 1739 – 1742 (1995).
18. C. Vanneste, P. Sebbah, and H. Cao, "Lasing with Resonant Feedback in Weakly Scattering Random Systems," Phys. Rev. Lett. **98**, 143,902/1–4 (2007).
19. P. Anderson, "Absence of Diffusion in Certain Random Lattices," Phys. Rev. **109**, 1492 – 1505 (1958).
20. N. M. Lawandy, R. M. Balachandran, A. S. L. Gomes, and E. Sauvain, "Laser action in strongly scattering media," Nature **368**, 436 – 438 (1994).
21. P. Sebbah and C. Vanneste, "Random laser in the localized regime," Phys. Rev. B **66**, 144,202/1–10 (2002).
22. M. N. Shkunov, M. C. DeLong, M. E. Raikh, Z. V. Vardeny, A. Zakhidov, and R. H. Baughman, "Photonic versus random lasing in opal single crystals," Synth. Metals **116**, 485 – 491 (2001).
23. M. Shkunov, Z. Vardeny, M. DeLong, R. Polson, A. Zakhidov, and R. Baughman, "Tunable, gap-state lasing in switchable directions for opal photonic crystals," Adv. Funct. Mater. **12**, 21–26 (2002).
24. S. Gottardo, R. Sapienza, P. D. García, A. Blanco, D. S. Wiersma, and C. López, "Resonance-driven random lasing," Nature Photon. **2**, 429–432 (2008).
25. A. Yariv, *Optical Electronics in Modern Communications*, 5th ed. (Oxford University Press, New York, 1997).
26. Y. Nishijima, K. Ueno, S. Juodkazis, V. Mizeikis, H. Misawa, T. T, and K. Maeda, "Inverse silica opal photonic crystals for optical sensing applications," Opt. Express **15**, 12,979–12,988 (2007).
27. H. Fujiwara and K. Sasaki, "Lasing of a microsphere in dye solution," Jpn. J. Appl. Phys. **38**, 5101 – 5104 (1999).
28. R. Polson, A. Chipouline, and Z. Vardeny, "Random lasing in $\pi-$conjugated films and infiltrated opals," Adv. Mater. **13**, 760–764 (2001).
29. R. Polson and Z. Vardeny, "Organic random lasers in the weak-scattering regime," Phys. Rev. B **71**, 045,205 (2005).
30. L. Teh, C. Wong, H. Yang, S. Lau, and S. Yu, "Lasing in electrodeposited ZnO inverse opal," Appl. Phys. Lett. **91**, 161,116 (2007).

1. Introduction

Photonic crystals [1, 2] hold promise for a new generation of optoelectronic devices exploiting photonic band gap (PBG) effect for the control over emission and propagation of optical radiation [3]. Photonic crystal-based laser radiation sources are expected to constitute an important part of photonic crystal-based optical circuits. Opal structure photonic crystals synthesized via self-organized sedimentation of monodisperse microspheres from liquid solutions [4] are easily available high-quality three-dimensional (3D) PBG materials [5, 6]. Although low refractive index contrast of as-fabricated structures prevents opening of 3D PBG, index contrast enhancement techniques were recently developed [7], allowing to convert them into high index contrast structures. In addition, fabrication of structural defects, such as linear waveguides in initially periodic opals, was successfully developed [8].

Modified spontaneous emission [9, 10, 11] and lasing [12, 13, 14, 15] from opal photonic crystal films with embedded gain media can add yet another functional capability useful for the formation of synthetic opal-based 3D optical circuits. The main difference between photonic crystal lasers and their conventional counterparts is absence of discrete optical cavity. In photonic crystals optical feedback generally occurs due to spatially distributed multiple scattering. Various feedback mechanisms related to disorder, multiple scattering, and Anderson localization [16, 17, 18, 19] were previously identified in various photonic systems. Lasing from opal photonic crystals is typically investigated by infiltrating them with liquid or solid gain media, such as dye solutions, or semiconductors. Previously, random [13, 20, 21] and

#99396 - $15.00 USD Received 25 Jul 2008; accepted 17 Aug 2008; published 20 Aug 2008

photonic lasing [12, 22, 23] were identified as the two main lasing regimes in synthetic opals. Random lasing is typically found in low index contrast opals, such as those consisting of silica or polystyrene (refractive index $n \approx 1.5$) nanospheres infiltrated by dye solutions with a close refractive index ($n \approx 1.3$). In these circumstances localization of light by periodic index modulation is inhibited, whereas small residual disorder leads to weak localization and formation of "random feedback" cavities, producing stochastic superposition of multiple lasing modes in the lasing spectrum. Random lasing always occurs at the peak of the gain band, and is independent of the photonic crystal periodicity [12] (however, resonant scattering effects can spectrally tune random lasing [24]). Photonic lasing is associated with distributed feedback (DFB) [25] due to periodic refractive index or gain modulation. Role of this lasing mechanism tends to increase with refractive index contrast, although photonic lasing due to periodic gain modulation is also observable at vanishing index contrast as well [12]. Photonic lasing [13] produces spectrally stable emission lines at the Bragg wavelength of the periodic structure. This feedback regime allows to obtain low-threshold single-mode lasing, and is most interesting for potential applications, despite the finding that lasing wavelength is fixed to the Bragg wavelength, defined by the distances between opal crystalline planes.

In this work we study lasing from zirconia (zirconium dioxide, ZrO_2) inverse opal structures, specially prepared for these studies and infiltrated by solutions of various organic dyes. Compared to other opal structures in which lasing was studied earlier, zirconia has higher refractive index $n_{ZrO_2} = 2.1$ and thus retains a considerable index contrast even when infiltrated by liquids with refractive index of $n \approx 1.3$. Large index contrast favors realization of index modulation coupled DFB regime. Small zirconia filling fraction in the inverse opal structure (about 26%) leaves 74% of the total volume available for the gain medium. Moreover, zirconia has a large optical damage threshold in excess of 100 GW/cm^2, which allows one conduct lasing tests in a wide range of pumping powers without irreversible damage to the underlying structure. Although lasing at lower pump levels is generally desired for applications, robust zirconia structures allow pumping of smaller sample areas (which requires higher pump fluences), leading to a modified lasing regime. As a result, we have observed stable single-mode photonic lasing from zirconia opals infiltrated by various rhodamine dyes. The lasing has spectral full width at half maximum (FWHM) of less than 1 nm, and quality factor of about 4000. In agreement with earlier findings, central wavelength of the photonic lasing does not coincide with the peak spontaneous emission wavelength. At the same time, the central wavelength is not fixed to the Bragg wavelength of the DFB resonator, but apparently depends on both the Bragg wavelength and the spontaneous emission peak position. This behaviour differs from the earlier reports on photonic lasing, and indicates the possibility of achieving modified photonic lasing in which lasing wavelength is tunable within the photonic stop band by spectral tuning of the emission band.

2. Samples and experimental details

Preparation of inverse zirconia opal samples generally followed the procedures described in our earlier work [26], except for inversion process which used a different material. In brief, polystyrene microspheres with diameter of 300 nm (Sekisui Plastics Co., Ltd.) were deposited on the cover glass substrates by centrifuged sedimentation at 5000 rpm for 10 min. Direct polystyrene opal template structures resulting from the self-organized sedimentation were subsequently dried and annealed at the temperature of 90 °C for 3 min. in order to produce moderate sintering of the spheres. Subsequently, the direct structures were infiltrated by zirconia using a low-temperature sol-gel procedure by immersion into $Zr(i\text{-}Pr)_4 : MeOH : HNO_3 = 1 : 1 : 0.1$ sol. After sintering of zirconia sol at 500 °C for 3 h, residual polystyrene was removed from the structures by washing in ethyl acetate. As a result, inverse zirconia opal films with total thick-

#99396 - $15.00 USD Received 25 Jul 2008; accepted 17 Aug 2008; published 20 Aug 2008

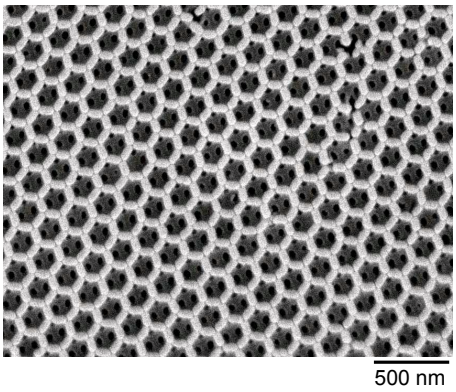

Fig. 1. SEM image of a (111) crystallographic plane of zirconia inverse opal structure.

ness of about 100 μm were obtained. Inspection of the samples was carried out by scanning electron microscopy (SEM). Figure. 1 shows SEM image of the top surface of the film, which is parallel to the substrate and to (111) crystallographic plane of face-centered cubic (fcc) structure. The SEM image illustrates good periodic ordering of the zirconia core regions, and indicates an average distance between the centers of neighboring air spheres of $d_{sphere} = 220$ nm. Since the original template was composed of polystyrene spheres with diameter of 300 nm, reduction of the lattice period by about 25% has most likely occured due to the sintering of the template and subsequently, due to shrinkage of the structure after zirconia infiltration. Nevertheless, these deformations have likely occurred uniformly across the entire sample, and their only significant result was the decrease in the lattice period. Planar stacking faults along the $\langle 111 \rangle$ direction are known to be the most common type of structural defects in opal structures. These defects typically emerge on the (111) surface of the opal, where they can be seen as characteristic lines [23]. Careful inspection of our samples by SEM has indicated that surface areas of about 1 mm in size were free of the stacking faults and had good long-range periodicity.

Optical gain media were introduced in the inverse zirconia opals by soaking them in ethylene glycol solutions of Rhodamine dyes. In particular, rhodamine B (RhB) 1.5 mM, rhodamine 6G (Rh6G) 0.5 mM, and sulfo-rhodamine (SRh) 2.0 mM solutions were infiltrated. The samples were mounted on an inverted microscope (IX-71, Olympus) equipped with a focusing lens with a magnification of 10 times and a numerical aperture of NA=0.5. Frequency-doubled radiation of a nanosecond Nd:YAG laser operating at the wavelength of 532 nm, repetition rate of 10 Hz, and having a temporal length of7 ns was used as a pump source. The laser beam was coupled into the microscope and focused on the sample by the objective lens. The emission was collected by the same objective lens, analyzed using a spectrometer with 2400 groves/mm grating (resolution ~ 0.1 nm), and recorded by a Peltier effect-cooled CCD detector. Spectral studies of lasing were performed repeatedly on different parts of the samples by translating the samples using a two-dimensional translation stage attached to the microscope. Diameter of of the pumped spot on the sample was maintained at about 30 μm by introducing a moderate divergence into the laser beam prior to the microscope. It is expected that the excited areas were structurally homogeneous, since their size on the surface was much smaller than typical size of defect-free surface area (about 1 mm). This setup allows excitation and probing of the optical emission in our samples along the $\langle 111 \rangle$ crystallographic direction. However, due to the numerical aperture of the objective, both excitation and signal collection was conducted within a conical range of incidence angles rather than normal to the (111) crystalline planes. This circumstance prevented studies of directional properties of the observed emission.

#99396 - $15.00 USD Received 25 Jul 2008; accepted 17 Aug 2008; published 20 Aug 2008

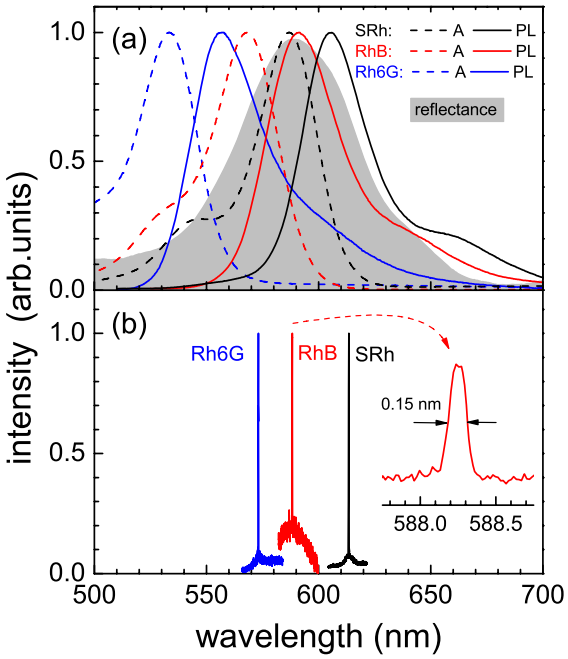

Fig. 2. (a) Peak-normalized PL (solid lines) and absorption (dashed lines) spectra of bulk sulfo-rhodamine (SRh), rhodamine B (RhB), and rhodamine 6G (Rh6G) solutions, with reflectivity spectrum of the inverse zirconia photonic crystal infiltrated by ethylene glycol solvent as a grey-shaded outline in the background (b) single-mode lasing spectra from zirconia inverse opal structures infiltrated by the dye solutions. The inset shows detailed shape and width of the lasing line for rhodamine B solution.

3. Results and discussion

Prior to the emission and lasing measurements, spectral positions of photonic stop bands along the $\langle 111 \rangle$ direction coincident to with normal to the opal film's surface was verified by reflectance measurements using the same optical setup as used for emission measurements and a halogen lamp as broadband irradiation source. In order to achieve the same refractive index contrast as in the lasing experiments, zirconia structures with refractive index of $n_{ZrO_2} = 2.1$ were soaked by pure ethylene glycol with refractive index of $n_{EG} = 1.42$. In these circumstances, inverse zirconia opals exhibit a photonic stop band centered at the 590 nm wavelength, as indicated by the pronounced reflectivity peak seen in Fig. 2(a). Bragg condition along the $\langle 111 \rangle$ leads to a high reflectance band centered at the wavelength

$$\lambda_{bragg} = 2d_{111}\sqrt{n_{eff}^2 - \sin^2(\theta)}, \tag{1}$$

where d_{111} is the distance between (111) crystalline planes and θ is the incidence angle. Effective refractive index n_{eff} is estimated as $n_{eff} = f_{sphere}n_{EG} + (1 - f_{sphere})n_{ZrO_2} = 1.6$, where f_{sphere}= 0.74 is the sphere volume filing ratio for closely packed opals. Since $d_{111} = 0.816 \cdot d_{sphere}$, $\lambda_{bragg} = 575$ nm can be estimated from (1). This value is close to the peak reflectivity wavelength seen in the experimental spectrum. It is helpful to stress here, that for normal

#99396 - $15.00 USD Received 25 Jul 2008; accepted 17 Aug 2008; published 20 Aug 2008

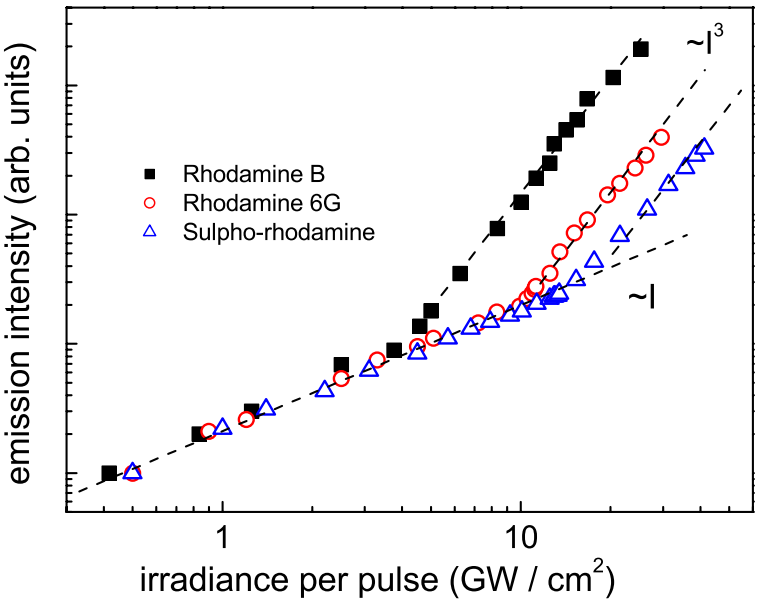

Fig. 3. Dependencies of the emission power on the pump irradiance demonstrating threshold-like emission.

incidence angle the pump wavelength of 532 nm is outside the reflectance band, and hence is not significantly attenuated due to the stop band.

Absorption and photoluminescence (PL) bands of bulk dye solutions intended for the infiltration (see Sect. 2) are shown in Fig. 2(a). As can be seen, for each dye solution absorption and PL bands form Stokes-shifted pairs. In all solutions except rhodamine 6G, absorption and PL bands are spectrally well overlapped with the photonic stop band. In rhodamine 6G, the absorption band lies on the short-wavelength edge of the stop band, but the Stokes-shifted PL band is still overlapped with it.

Figure 2(b) shows the measured emission spectra from dye-infiltrated samples under intense optical pumping by the laser. The spectra are dominated by single narrow peaks riding on a somewhat weaker and broader background emission bands. The peaks, whose spectral half-width does not exceed 1.0 nm in all dyes and for a wide range of pump intensities, emerge above certain threshold pump power levels, depending on the dye. Inset in Fig. 2(b) shows the detailed shape of lasing mode just above the threshold in a structure infiltrated by rhodamine B. The measured spectral width of the emission (≈ 0.15 nm) is close to the resolution limit of the spectrometer $\sim 0.1-0.2$ nm, indicating that the lasing mode may actually be even more narrow. Accordingly, the mode quality factor $Q=\Delta\lambda/\lambda_{max}$ of about $Q=4000$ can be estimated for the measured peak, but the actual quality factor may be higher. These quality factors can be regarded as large for 3D structures fabricated by self-organization and template inversion.

Figure 3 shows the measured spectrally-integrated emission power dependencies on the pump irradiance. These dependencies consist of linear and super-linear parts. The linear parts mainly reflect power dependencies of spectrally broad background, since the narrow peaks are

#99396 - $15.00 USD Received 25 Jul 2008; accepted 17 Aug 2008; published 20 Aug 2008

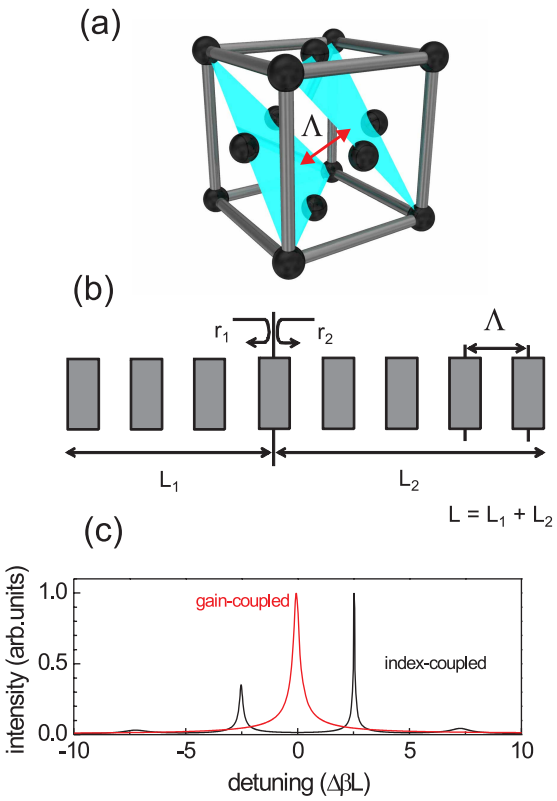

Fig. 4. (a) Schematic representation of fcc opal crystalline cell with $\langle 111 \rangle$ planes outlined, (b) one-dimensional model of of the corresponding distributed laser cavity filled by material(s) with periodically modulated refractive index and optical gain, lengths (L_1, L_2) and reflection coefficients (r_1, r_2) are defined in accordance with literature [25], (c) dependencies of the lasing intensity versus detuning in the frequency domain $(\Delta\beta L)$ from the Bragg frequency $\omega_0 = \frac{\pi c}{\Lambda n}$, calculated using theory given in the literature [25].

absent in this regime. Transitions to super-linear dependency in each case occur mainly due to threshold-like appearance of the spectrally narrow, intense peak. The spectra shown in Fig. 2(b) were recorded at pump levels exceeding the respective thresholds by 10%. However, the peak wavelengths and spectral widths were found to be independent of the pumping power, thus indicating negligible role of optical nonlinearities (either in the dye solution and in the zirconia). The emission lines were also found to be invariant to angular tuning, which was performed by tilting the sample at angles of up to 20^0 with respect to the optical axis of the measurement setup. Generally, these observations allow interpretation of the narrow emission peaks as single-mode lasing.

Several optical feedback mechanisms were identified previously in photonic crystal structures exhibiting lasing. Random lasing [27, 21] occurs due to optical feedback related to multiple random scattering, and is spectrally seen as random superposition of narrow lasing lines [28, 29]. In opal photonic crystals random lasing always occurs at the peak of the PL band and is not related to the spectral position of photonic stop band [12]. Another likely mechanism is so-called photonic lasing, which occurs due to optical feedback originating from multiple reflections in periodic structures. Under moderate pumping, photonic lasing in opals typically

#99396 - $15.00 USD Received 25 Jul 2008; accepted 17 Aug 2008; published 20 Aug 2008

occurs as a single, spectrally narrow peak at the Bragg wavelength, and does not necessarily coincide with the peak emission in the PL band [12, 22]. Within the class of photonic lasing, further distinction can be made between the subclasses of gain-coupled and refractive index modulation-coupled distributed feedback (DFB) regimes. Figure 4(a) shows schematically an fcc cell of opal photonic crystal with $\langle 111 \rangle$ crystallographic planes separated by the distance $\Lambda = d_{111} = 0.816 d_{sphere}$. Periodic sequence of parallell planes can be represented by a simple one-dimensionally periodic discrete structure with period Λ shown schematically in Fig. 4(b). Operation of DFB-based lasers in the simple one-dimensional case is well-studied in the existing literature [25]. Figure 4(c) shows normalized lasing spectra obtained from analytical expressions given in [25] for gain-coupled and refractive index modulation-coupled feedback regimes. As can be seen, gain-coupled DFB lasing always occurs at Bragg wavelength, whereas for the index modulation-coupled DFB regime oscillations at Bragg wavelength are forbidden due to symmetry of the system, and two modes detuned by $\omega_{1,2} = \pm \frac{\pi c}{\Lambda n L}$ from the Bragg frequency are observed. In practically used one-dimensional DFB lasers this condition is typically lifted by introduction of symmetry-breaking defects, and single mode at Bragg frequency can be observed. In 3D systems like inverse opal studied in this work, this condition may be relaxed due to three-dimensional character of the structure and due to inherent asymmetry of the optically pumped 3D region. However, in any case the emission wavelength of DFB lasers is fixed with respect to the Bragg wavelength and the photonic stop band.

The lasing behavior observed in this study matches some, but not all of the established features of photonic lasing, and at the same time appears to be quite different from the random lasing regime. Below we briefly summarize its main features in comparison to these well-studied cases.

Role of lattice periodicity. The observed lasing depends on the lattice periodicity. This conclusion is supported by additional experiments, in which presence of lasing from inverse zirconia opals was verified using dyes whose PL bands are outside the photonic stop bands. Observation of lasing in this case would indicate a feedback mechanism that is independent of the lattice periodicity, similar to random lasing. However, no lasing was observed at equivalent pumping levels.

Position of the lasing peak with respect to PL band maxima. As is evident from Fig. 2(a), the lasing does not necessarily occur at the peak of PL band (although lasing line and the PL peak almost coincide for rhodamine B). This feature also indicates similarity to photonic lasing.

Position of the lasing peak with respect to the reflectance band of photonic crystal. The lasing occurs at different spectral positions within the stop band, depending on the PL band position. This feature differs from the known features of classical DFB lasing, where emission always occurs as single or double peaks at the Bragg wavelength (i.e.,center of the photonic stop band).

Angular invariance. As noted above, the lasing lines were found to be spectrally invariant to moderate tilting of the sample. It is important to stress, that previous studies [23] have demonstrated angular tunability of the photonic lasing lines within the stop gap region, which was explained by varying orientation of the stacking fault defects with respect to the lasing direction, and the corresponding spectral tuning of defect states. In this study, the excited area is smaller, and is most likely defect-free. Moreover, both pumping and observation are conducted along a range of directions falling within the conical acceptance angle of the microscope lens. Hence, spectral dependence is unlikely, and our observations do not contradict the earlier findings.

Thus, lasing from the inverse zirconia opals is essentially similar to the photonic lasing identified earlier [22]. However, in our case the lasing wavelength is not fixed to the Bragg wavelength, but is tunable within the photonic stop band. On the other hand, the lasing wavelength does not coincide spectrally with the peak PL intensity. Generally, lasing occurs at wavelengths

#99396 - $15.00 USD Received 25 Jul 2008; accepted 17 Aug 2008; published 20 Aug 2008

that appear to be correlated to both the stop gap reflectivity and the PL bands. In these circumstances spectral tuning of the lasing line is possible via spectral tuning of the PL band. In our experiments tuning is realized by simply exchanging the active dye, but other active materials, such as semiconductors [30] may allow reversible tuning of the emission band and the lasing wavelength.

4. Conclusions

We have fabricated 3D zirconia inverse opal photonic structures, and have investigated lasing properties of these structures infiltrated by liquid solutions of rhodamine dyes. Zirconia inverse opals have larger refractive index, are mechanically and optically more robust than as-fabricated polystyrene direct opals, and under intense optical pumping can withstand irradiances up to the $\sim$ 100 GW/cm^2 level. Under intense pumping we have observed stable single-mode photonic lasing at wavelengths that fall within the high reflectance photonic stop band associated with periodicity of the $\langle 111 \rangle$ opal planes. At the same time, the lasing wavelength does not match neither the Bragg wavelength of the periodic structure nor the peak of the dye spontaneous emission band. Spectral width and quality factor of the lasing lines are about 1 nm (FWHM), and 4000, respectively. Although this regime of photonic lasing is achieved at relatively high pump irradiance levels in our experiments, it demonstrates an interesting possibility of obtaining single-mode lasing with wavelength tunable around the Bragg wavelength. More detailed experimental and theoretical investigations are needed future in order to clarify the feedback and tuning mechanisms, as well describe directional and polarization properties of the lasing.

Acknowledgments

This work was supported by funding from the Ministry of Education, Culture, Sports, Science, and Technology of Japan: KAKENHI Grant-in-Aid (No. 19049001) for Scientific Research on the Priority Area “Strong Photon-Molecule Coupling Fields for Chemical Reactions” (No. 470), Grant-in-Aid from Hokkaido Innovation through Nanotechnology Support (HINTS), and Grant-in-Aid for JSPS Fellows. The authors are grateful to Dr. Hideki Fujiwara at the Research Institute for Electronic Science (RIES), Hokkaido University, for useful discussions.

#99396 - $15.00 USD Received 25 Jul 2008; accepted 17 Aug 2008; published 20 Aug 2008